Elastic Constants of and Wave Propagation in Antimony and Bismuth

SEYMOUR EPSTEIN AND A. P. DEBRETTEVILLE, JR.
U. S. Army Electronics Laboratories, Fort Monmouth, New Jersey
(Received 5 November 1964)

Ultrasonic wave velocities for 14 different modes were obtained on two differently oriented single-crystal antimony cubes from the time between successive unrectified radio-frequency pulse echoes. This redundant set of data was fitted by a least-squares technique to Voigt theory to yield the six room-temperature adiabatic elastic-stiffness constants. In units of 10^{10} dyn/cm^2, $c_{11}=99.4(1)$, $c_{33}=44.5(9)$, $c_{44}=39.5(5)$, $c_{66}=34.2(3)$, $c_{13}=26.4(4)$, and $c_{14}=+21.6(4)$, the positive sign for c_{14} following from our choice of positive Cartesian axes. When similarly treated, Eckstein, Lawson, and Reneker's bismuth data yield in these same units: $c_{11}=63.22$, $c_{33}=38.11$, $c_{44}=11.30$, $c_{66}=19.40$, $c_{13}=24.40\pm0.09$, $c_{14}=+7.20$. Also included are a visual method of fixing the laboratory coordinate system in antimony by means of an imperfect cleavage plane, a calculation of the pure-mode directions in the mirror plane, a simple formula for choosing the nonextraneous value of c_{13} for trigonal crystals having six independent elastic constants without resorting to lattice-stability criteria, and a calculation of the deviation of elastic-wave particle displacement and energy-flux directions from the propagation direction. For waves propagating in the (0,1,1) and (0,$\bar{1}$,1) directions, the particle-displacement deviations for antimony and bismuth do not exceed 15° and 13°, respectively, and corresponding energy-flux deviations up to 45° and 27° are obtained.

I. INTRODUCTION

IN the well-designed experiment of Eckstein, Lawson, and Reneker[1] (hereinafter referred to as ELR), trigonal bismuth's six adiabatic elastic stiffness constants were determined from measurements of acoustic-wave propagation. An extension of their work to antimony seemed natural, and a recently determined set of antimony constants is desirable, considering both (1) the fact that currently available antimony crystals are purer and less strained than those available to Bridgman[2] and (2) the different measuring technique. The design of our experiment is essentially that of ELR, but our data are principally taken on just two differently oriented specimens, and our method of calculating the elastic constants differs in that we use a least-squares procedure. (For completeness and clarity of presentation we incorporate the basic data and equations given by ELR, and other material as appropriate; the reader is nevertheless referred to ELR for points not covered, and for additional references.) In addition, an inspection method of establishing laboratory axes in antimony is described; a simple formula is given for obtaining the nonextraneous value of c_{13}; the directions of pure-mode propagation in the mirror plane are evaluated; and the directions of particle displacement and energy flux for certain modes are calculated and compared with the wave-propagation direction. ELR's 14 bismuth velocities are also reanalyzed by our procedures, and a comparison between the two similar elements is made.

In the next section of this paper, some well-known crystallographic and cleavage data for antimony are introduced to provide a background for presenting the convention used for choosing coordinate axes in the crystal. This is followed by sections on the design of the experiment, experimental detail and the method of calculation of the constants. In the remaining sections the limitations of our analysis, the elastic constants, and acoustoelastic wave-propagation properties in anisotropic antimony and bismuth are discussed.

II. CRYSTALLOGRAPHIC DATA AND CLEAVAGE PROPERTIES OF ANTIMONY

Like bismuth, antimony's primitive cell is a 2 atom/cell rhombohedron (Fig. 1) with one atom at each corner and a ninth slightly displaced from the midpoint in the (1,1,1) direction. The nearest-neighbor distances[3] are 2.87 and 3.37 Å, the density is 6.7 g/cm^3, the rhombohedral angle is 57°6′, and the cell edge is 4.49 Å at room temperature.[4] It is brittle. The principal cleavage plane at room temperature is the (111) plane and fracture occurs between atoms having the larger nearest-neighbor distance; the secondary cleavage plane is of the (211) type indexed in the primitive cell,[5,6] and is relatively imperfect. These latter planes, spoken of as dominant secondary cleavage planes by one of us,[7] intersect the (111) plane in lines giving the directions of the three equivalent twofold axes. These axes are normal to the mirror planes which contain the trigonal and bisectrix axes. The plane's position in relation to a right-handed Cartesian coordinate system fixed in the crystal, or what is equivalent, the position of the plane's Laue spot reflection, can be used (see Sec. IV) to distinguish between two possible choices for such coordinate systems in which the signs of c_{14} and certain magnetoresistance coefficients[7] change. Our choice of coordinate system and the convention used to choose it

[1] Y. Eckstein, A. W. Lawson, and D. H. Reneker, J. Appl. Phys. **31**, 1535 (1960).
[2] P. W. Bridgman, Proc. Am. Acad. Arts Sci. **60**, 365 (1925).
[3] W. L. Bragg, *Atomic Structure of Minerals* (Cornell University Press, Ithaca, New York, 1937).
[4] C. S. Barret, P. Cucka, and K. Haefner, Acta Cryst. **16**, 451 (1963).
[5] C. Palache, H. Berman, and C. Frondel, *Dona's System of Mineralogy* (John Wiley & Sons, Inc., New York, 1955), Vol. 1.
[6] Relative to a hexagonal cell, this plane is of the (10$\bar{1}$4) type. Referred to a larger eight-atom-containing nearly face-centered cubic cell, it is of the (011) type (also shown in Fig. 1).
[7] Seymour Epstein, J. Electrochem. Soc. **109**, 738 (1962); Seymour Epstein and H. J. Juretschke, Phys. Rev. **129**, 1148 (1963).

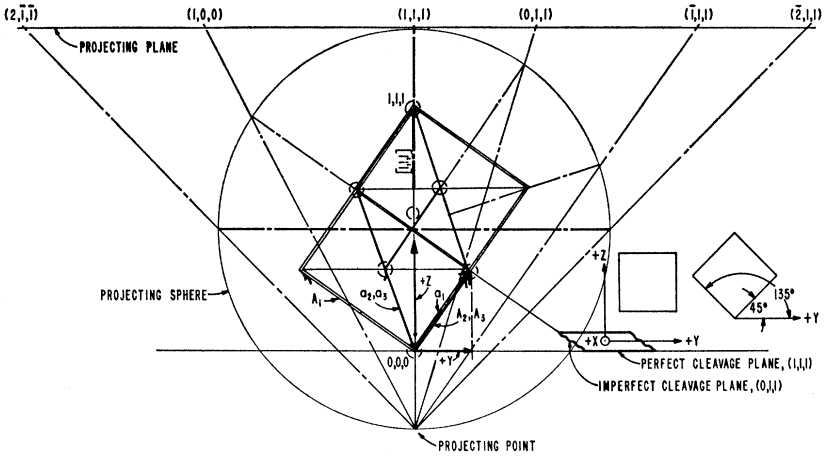

FIG. 1. Primitive and nearly cubic rhombohedral cells, stereogram of ⟨011̄⟩ zone (normal to the page) of the nearly cubic cell, specimen orientation and positive-sensed Cartesian axes, and position of two pronounced cleavage planes of antimony. a_1, a_2, and a_3 are the rhombohedral-cell axis vectors for the primitive cell and the outward direction of the projection of any one of them, a_1 for example, on a plane normal to the unique [111] direction is taken as $+Y$. $a_1+a_2+a_3$ is chosen as $+Z$. A_i are the cell edges of the nearly cubic cell. $+Y$ is along $(\bar{2},1,1)$ and $+X$ along $[01\bar{1}]$.

are arbitrary. So that the signs of c_{14} for antimony and bismuth can be directly compared, we adopt ELR's specification for the positive-axes senses, as shown in Fig. 1.

The axes senses in the specimens were determined upon indexing a Laue diagram. (See Sec. IV.)

III. DESIGN OF EXPERIMENT

As outlined by ELR and their cited references, the six Voigt elastic stiffness constants for the class $R\bar{3}m$ are represented by

$$c_{ij}=\begin{vmatrix} c_{11} & c_{12} & c_{13} & c_{14} & 0 & 0 \\ c_{12} & c_{11} & c_{13} & -c_{14} & 0 & 0 \\ c_{13} & c_{13} & c_{33} & 0 & 0 & 0 \\ c_{14} & -c_{14} & 0 & c_{44} & 0 & 0 \\ 0 & 0 & 0 & 0 & c_{44} & c_{14} \\ 0 & 0 & 0 & 0 & c_{14} & c_{66} \end{vmatrix},$$

where $c_{66}=(c_{11}-c_{12})/2$. For acoustoelastic waves propagating with direction cosines l, m, n, in this order relative to the X, Y, and Z axes of a right-handed coordinate system, three values for the velocities (one longitudinal and two transverse) satisfy the Christoffel determinant. Symmetry, however, prevents one from choosing six of the nine possible modes which would allow the direct (and accurate) determination of the six constants on one simply shaped oriented specimen. Consequently, it is necessary to employ a minimum of two differently oriented single-crystal cubes and more than the minimum of six modes required in principle to determine six constants. All but c_{13} are best arrived at when (1) they derive from velocities of three modes propagating along each coordinate-axis direction on one specimen and (2) the velocity data so obtained are self-consistent. Accordingly, one of the two specimens needed is a cube with faces normal to the principal axes. To determine c_{13} symmetry requires one to employ a mode propagating at any angle with the trigonal axis other than 0°, 90°, and 180° (plus four of the five previously discussed constants). Two directions (45° and 135° with the Y axis in the Y-Z mirror plane) exist for which c_{13} makes its maximum contribution to the effective stiffness constant, and our second cube is oriented with faces normal to these directions and normal to the X direction. To insure that the five already determined values for the constants are the same for this cube, velocity data are obtained for its nine possible modes.

In all, 18 velocity measurements are required. Because one of them corresponds to a doubly degenerate shear mode along the Z axis, and three others repeat the modes along the X axis on the second orientation, only 14 velocities need be analyzed in detail. Clearly, these must satisfy 8 redundancy relations for a meaningful calculation of the six elastic constants. The 14 expressions for the effective stiffness constants ρv_i^2 are listed in Table I. (The symbols v_1 through v_{14} are chosen to correspond to ELR's arbitrary assignment.) Also included are the wave-propagation and transducer-polarization-direction cosines, the numerical values of the averaged observed velocities, and the experimental tolerances.

IV. EXPERIMENTAL DETAIL

The velocity of sound was determined by the ultrasonic pulse-echo method. A pulse width of approximately 2 μsec wide was used and the distance between the maximum amplitude of successive unrectified radio-frequency pulses was used as a measure of the transit time.[8] Transit-time error effects were also investigated by means of the dummy-transducer method.[9] Times were measured on a Tektronix 585A oscilloscope whose timing circuit was checked with a counter (Hewlett-Packard 524B) and a quartz signal generator (Tektronix Time Marker Generator 180-S1). An Arenberg PG-65-C pulse generator, preamplifier PA-620-B, and wideband amplifier WA-600-B were used to generate and amplify the pulses. An X- or Y-cut-quartz transducer of 10- or 5-Mc/sec fundamental frequency func-

[8] S. Eros and J. R. Reitz, J. Appl. Phys. **29**, 683 (1958).
[9] C. S. Smith and J. W. Burns, J. Appl. Phys. **24**, 15 (1953).

TABLE I. Effective stiffness constant equations and experimental antimony velocities.

Eq. No.	Effective stiffness constant equations (ρ, the material density)	Direction cosines of propagation vector	Direction cosines of transducer polarization	Experimental velocity 10^5 cm/sec
(1)	$\rho v_1^2=c_{11}$	100	100	3.92±2%
(2)	$\rho v_2^2=\frac{1}{2}[(c_{66}+c_{44})+\{(c_{44}-c_{66})^2+4c_{14}^2\}^{1/2}]$		001	3.00±1.5%
(3)	$\rho v_3^2=\frac{1}{2}[(c_{66}+c_{44})-\{(c_{44}-c_{66})^2+4c_{14}^2\}^{1/2}]$		010	1.53±2.6%
(4)	$\rho v_5^2=c_{66}=\frac{1}{2}(c_{11}-c_{12})$	010	100	2.23±1.5%
(5)	$\rho v_4^2=\frac{1}{2}[(c_{11}+c_{44})+\{(c_{44}-c_{11})^2+4c_{14}^2\}^{1/2}]$		010	3.98±1.7%
(6)	$\rho v_6^2=\frac{1}{2}[(c_{11}+c_{44})-\{(c_{44}-c_{11})^2+4c_{14}^2\}^{1/2}]$		001	2.24±2%
(7)	$\rho v_7^2=c_{33}$	001	001	2.60±1.2%
(8)	$\rho v_8^2=c_{44}$		100 or 010	2.45±1.2%
(9)	$2\rho v_9^2=\frac{1}{2}(c_{11}+c_{33})+c_{44}-c_{14}$ $+\{(\frac{1}{2}c_{11}-\frac{1}{2}c_{33}-c_{14})^2+(c_{13}+c_{44}-c_{14})^2\}^{1/2}$	0, $1/\sqrt{2}$, $1/\sqrt{2}$	0, $1/\sqrt{2}$, $1/\sqrt{2}$	3.12±1.9%
(10)	$2\rho v_{11}^2=\frac{1}{2}(c_{11}+c_{33})+c_{44}-c_{14}$ $-\{(\frac{1}{2}c_{11}-\frac{1}{2}c_{33}-c_{14})^2+(c_{13}+c_{44}-c_{14})^2\}^{1/2}$		0, $-1/\sqrt{2}$, $1/\sqrt{2}$	1.25±1%
(11)	$\rho v_{10}^2=\frac{1}{2}(c_{66}+c_{44})+c_{14}$		100	2.87±4.1%
(12)	$\rho v_{13}^2=\frac{1}{2}(c_{66}+c_{44})-c_{14}$	0, $-1/\sqrt{2}$, $1/\sqrt{2}$	100	1.54±10%
(13)	$2\rho v_{12}^2=\frac{1}{2}(c_{11}+c_{33})+c_{44}+c_{14}$ $+\{(\frac{1}{2}c_{11}-\frac{1}{2}c_{33}+c_{14})^2+(c_{13}+c_{44}+c_{14})^2\}^{1/2}$		0, $-1/\sqrt{2}$,$1/\sqrt{2}$	4.14±1.8%
(14)	$2\rho v_{14}^2=\frac{1}{2}(c_{11}+c_{33})+c_{44}+c_{14}$ $-\{(\frac{1}{2}c_{11}-\frac{1}{2}c_{33}+c_{14})^2+(c_{13}+c_{44}+c_{14})^2\}^{1/2}$		0, $1/\sqrt{2}$, $1/\sqrt{2}$	1.50±6%

tioned as the transmitting and receiving transducer. Measurements were taken between 5 and 70 Mc. The frequency which gave the sharpest pattern for a particular mode is the one at which the velocity was measured. These best frequencies were scattered throughout this range. More than one frequency gave a decipherable pattern for a given mode, but most frequencies did not. It was, however, possible to obtain a crude check of the frequency dependence of v_7. This result together with qualitative results for other modes at two frequencies show no frequency dependence within the specified experimental tolerances.

Salol was used to bond the transducer to the specimen surface which was either a natural cleavage surface, the (111) plane, for slab specimens, or a comparatively rougher spark-cut surface for the two specimens whose velocities were actually used to obtain the constants. The slab specimens, cleaved at opposite faces and of varying thickness and width, were used primarily to check the effect of spark-cut surfaces on the coupling of energy into and out of the specimens and on the reflection of energy at the back surface into the specimen. No deleterious effects of spark cutting were seen. Another experimental check is that our values for v_1, v_4, and v_7 are within 4% of Eckstein's[10] 77°K velocities which are, respectively, 3.85, 4.08, and 2.58 10^5 cm/sec.

Zone-refined antimony, Cominco Grade 69, 99.999% pure, was the stock for our slabs and cubes. (Initially, stock which was very likely less pure was used and at the few points where checks were made yielded essentially the same results.)

The two differently oriented single-crystal cubes, 12 mm on edge, were prepared by spark cutting[11] their faces within ±1°, as required for our experimental design. Strains were checked for by x-ray diffraction.

Back-reflection Laue diagrams were used to choose the positive X, Y, and Z axes directions. They were indexed by identifying spots belonging to the $\langle 01\bar{1}\rangle$ zone (in the mirror plane) on each side of the (111) pole (see Fig. 1)—in particular, the $(3\bar{1}\bar{1})$, $(4\bar{1}\bar{1})$, $(5\bar{1}\bar{1})$, (100), (011), and $(\bar{1}11)$ spots. (These indices are based on the large, nearly cubic, rhombohedral cell containing 8 atoms; the notation is Vickers.)[12]

Part of Vickers' stereogram is reconstructed in Fig. 1 in order to show the relative positions of the secondary cleavage plane to the axes. This plane was positively identified by comparing the angle between the secondary cleavage plane and the (111) plane as measured on cleaved specimens, firstly with the estimated angle the (011) spot makes with the (111) spot, and next with the value for this angle given by Dana.[5] Our observations of secondary cleavages on many antimony rods and slabs show this plane to be easily observable and to slant in a unique direction. Accordingly, a convenient way of identifying the right-handed coordinate system used in the crystal is shown in Fig. 1. With the planes sloping downward to the right, the positive Y axis is directed from left to right, positive X toward the observer, and positive Z upward.

V. EXPERIMENTAL ANALYSIS AND RESULTS

Our velocity values, shown in Table I, represent averages of the average velocity calculated from meas-

[10] Y. Eckstein, Phys. Rev. **192**, 12 (1963).

[11] H. J. Ehlers, D. F. Kolesar, Rev. Sci. Instr. **34**, 1054 (N) (1963).

[12] W. Vickers, J. Metals **9**, 827 (1957).

urements of the time between successive echoes made over periods of weeks. They are rounded off to the last significant figure and the tolerances represent the larger of the fluctuations in these or the accuracy of a specific measurement. Transit-time errors attributable to the transducer, determined after all the velocity data were completed, are about 1%. They are not applied because (1) they could not be systematically obtained, (2) except for v_9's they are less than the over-all velocity tolerances specified for each velocity, and (3) we have no information on the fluctuations in the transit-time correction measurements themselves. Taken at face value, a 1% average correction to the velocities would scale the antimony stiffness values by 2%.

Before the numerical evaluation of the constants was carried out, the general features of the velocity data were examined for consistency with the equations of Table I as follows: v_{10} being greater than v_{13} clearly fixes c_{14} as positive for the axes senses chosen. In turn, this requires that $v_{12}^2+v_{14}^2$ be greater than $v_9^2+v_{11}^2$; $v_2^2>v_{10}^2$; $v_{13}^2>v_3^2$; and $v_{12}^2>v_9^2$, which is indeed the case within experimental error. These inequalities are compatible with assigning the larger velocity value of two coupled modes, normally associated with the longitudinal mode, to the positive radical of the relevant expressions, i.e., in the pairs v_2 and v_3, v_4 and v_6, v_9 and v_{11}, and v_{12} and v_{14}, the first velocity is the greater one. Next, the eight redundancy relations, a more sensitive and detailed test of the data than the trace relations used by ELR, were evaluated; one obtains that $v_{11}=1.25\pm1\%$ for antimony is incompatible with the others in this formalism. Consequently, attempts to fit to it and its inclusion in a least-squares function are meaningless and it is ignored in our calculation of antimony's constants. A possible reason for v_{11}'s incompatibility is discussed in the section on elastic-wave refraction.

Generally stated, our least-squares procedure is based on adjusting each of the 14 squares of the velocities within experimental error so that they give a minimum deviation from the central experimental-velocity-squared values and, when inserted in Eqs. (1) through (14), yield a common value for each of the six stiffness constants.

The least-squares function used is

$$F=\sum_{i=1}^{14}\left(\frac{v_{ia}^2-v_{io}^2}{2v_{io}\Delta v_i}\right)^2,$$

where the subscripts a and o signify adjusted and observed, and Δv_i is the experimental uncertainty in the ith velocity. This task is simplified by initially selecting those velocities and combinations of velocities which are related to the smallest number of stiffness constants and then extending the selection in steps to include more and more velocities until all the constants are obtained. As more velocities are included, the previously obtained values are readjusted when necessary. Specifically, first v_5^2, v_8^2, $v_{10}^2+v_{13}^2$, and $v_2^2+v_3^2$ are adjusted and c_{44} and c_{66} obtained. With these values and $v_{10}^2-v_{13}^2$ and $v_2^2-v_3^2$, a common value for c_{14} is obtained, usually upon readjustment of the previously obtained velocities and constants. After this, c_{11} is similarly obtained but from v_1^2, $v_4^2+v_6^2$, and $(v_4^2-v_6^2)^2$, and c_{33} from v_7^2, $v_9^2+v_{11}^2$, and $v_{12}^2+v_{14}^2$. Finally c_{13} is obtained from $(v_9^2-v_{11}^2)^2$ and $(v_{12}^2-v_{14}^2)^2$, again readjusting the already obtained values as necessary. Because each of the functions from which c_{13} is calculable yields two values, the common one is, of course, the proper one. (Antimony calculations involving incompatible v_{11} are omitted.)

The results of this procedure for antimony and for the complete bismuth data of ELR, and the results of other workers and their procedures, are presented in Tables II, III, and IV. These are next discussed.

VI. DISCUSSION

A. Nature and Limitations of Fit

In the course of fitting the antimony data, it became clear that the 14 equations of Table I intersect in a well-defined region of a 6-dimensional stiffness-constant space and that only a very narrow range of values for the constants is possible. The bounding limits of this region are, roughly, such that a change greater than 5% in almost any constant appears sufficient to bring one or more of the 14 velocities outside the experimental range. Accordingly, the basis for choosing the constants

TABLE II. Elastic stiffness constants at room temperature.

	c_{11}	c_{12}	c_{13}	c_{14}	c_{33}	c_{44}	c_{66}	Source
Sb	99.4(1)	30.9(1)	26.4(4)	+21.6(4)	44.5(9)	39.5(5)	34.2(5)	This work, least squares
	99.31				44.59			Eckstein,[a] transmission technique at 77°K
	81.00	11.00		+18.00	43.60	33.60	35.00	Leventhal,[b] echo technique
	79.20	24.70	26.10	+11.00	42.70	28.50	27.30	Bridgman,[c] static technique
Bi	63.22	24.42	24.40 ±.09	+ 7.20	38.11	11.30	19.40	ELR,[d] least-squares recalculation
	63.50	24.70	24.50	+ 7.23	38.10	11.30	19.40	ELR,[d] transmission technique
			21.50	+ 7.20				Kor's,[e] recalculation of ELR
	62.90	35.00	21.10	− 4.23	44.00	10.84	13.37	Bridgman,[c] static technique

Units: 10^{10} dyn/cm^2.

[a] See Ref. 10. [b] See Ref. 13. [c] See Ref. 2. [d] See Ref. 1. [e] See Ref. 14.

TABLE III. Elastic compliance constants at room temperature.

	S_{11}	$-S_{12}$	$-S_{13}$	$-S_{14}$	S_{33}	S_{44}	S_{66}	Source
Sb	16.2	6.1	5.9	12.2	29.5	38.6	44.6	This work, least squares
	17.7	3.8	8.5	8.0	33.8	41	43	Bridgman[a]
Bi	25.74	8.01	11.35	21.50	40.77	115.90	67.51	ELR,[b] least-squares recalculation
	26.9	14.0	6.2	−16.0	28.7	104.8	81.2	Bridgman[a]

Units: 10^{-13} cm²/dyn.

[a] See Ref. 2. [b] See Ref. 1.

TABLE IV. Calculated and experimental limits of velocities.

	Sb			Bi			
	Lower exp limit	Least-squares calculation	Upper exp limit	Lower exp limit	Least-squares calculation	ELR calculation	Upper exp limit
v_1	3.84	3.85(2)	4.00	2.518	2.540	2.545	2.562
v_2	2.95	2.96(0)	3.04	1.541	1.552	***1.635***	1.559
v_3	1.49	1.50(1)	1.57	0.851	0.851	***0.667***	0.859
v_4	3.91	3.98(5)	4.05	2.553	2.559	2.565	2.589
v_5	2.20	2.26(0)	2.27	1.398	1.407	1.406	1.416
v_6	2.19	2.20(4)	2.28	1.016	1.026	1.026	1.028
v_7	2.57	2.58(0)	2.63	1.957	1.971	1.571	1.987
v_8	2.42	2.43(0)	2.47	1.063	1.073	1.073	1.085
v_9	3.06	3.17(0)	3.18	2.063	2.067	2.109	2.101
v_{10}	2.75	2.95(6)	2.98	1.505	1.517	1.518	1.539
v_{11}	1.24	***1.86(6)***	1.26	1.144	1.147	***1.071***	1.156
v_{12}	4.06	4.17(5)	4.21	2.400	2.437	***2.491***	2.482
v_{13}	1.38	1.50(9)	1.69	0.907	0.912	0.910	0.913
v_{14}	1.41	1.56(2)	1.59	1.049	1.508	***0.937***	1.061

Units: 10^5 cm/sec.

was relaxed to obtaining a near-least-squares minimum fit. We estimate our values, presented in Table II, to be within about ±2% of a true least-squares minimum fit and we note that such a fit would be as uneven as the fit presented.

When applied to ELR's bismuth data, our procedure yields essentially one set of constants except for c_{13} which may range within ±0.09 of the value given without causing any one velocity to be calculated outside its experimental limit. That one set of values obtains is readily evident from the facts that our values differ little from ELR's, yet five of their calculated velocities are outside the experimental range and just one of ours is at the lower experimental limit. This fit is characterizable as even and quite good, considering the very small velocity tolerances ELR specify.

B. Comparison of Constants and Direct Calculation of c_{13}

Included in Table II with our constants are c_{11} and c_{33} calculated from Eckstein's[10] 77°K velocity data for antimony, ELR's bismuth constants values, bismuth and antimony values calculated from Bridgman's[2] early isothermal compliance measurements, unpublished antimony values of Leventhal[13] and some calculated bismuth values of Kor.[14] Agreement with Eckstein's c_{11} and c_{33} for antimony has already been pointed out in Sec. IV (by noting that his v_1 and v_7 and ours are the same); and except for c_{11}, agreement with Leventhal is fair. Although the nature of our original stock and our method of preparation are preferable to Leventhal's, we cannot account for the discrepancies on the basis that our crystals are purer and less strained. We have already noted that v_7 and v_8 were also obtained on cleaved surfaces and that these values agreed well with the values obtained on our cube. The purity of the cleaved specimen was less than that of the cube (although very likely still purer than Leventhal's). Furthermore, v_9 and v_{11} were again measured after the specimen was (accidentally) damaged. A 3-mm transducer was placed next to the cracked region where no visible signs of damage were obvious; no change in the velocity values were found.

Our recalculation of the bismuth constants yields essentially ELR's values within about 1% or less. Compared to Bridgman's results, our individual constants fit poorly for both antimony and bismuth, even allowing for the large cumulative error introduced for some of the constants by the inverse tensor transformation and the negligibly small isothermal corrections. Uniform and over-all agreement is not necessarily to be expected since some of his individual values are adjusted to fit his linear and volume compressibilities. On the other hand, the compressibilities calculated from our data do agree with his directly measured unadjusted compressi-

[13] E. Leventhal, MS thesis, Polytechnic Institute of Brooklyn, New York, 1959 (unpublished).
[14] S. K. Kor, Physica 28, 837 (1963).

TABLE V. Linear and volume compressibilities. Units: 10^{-13}cm^2/dyne.

	Sb		Bi	
	This work	Bridgman[a] (Ref. 2)	ELR, recalculated	Bridgman[a] (Ref. 2)
k_t	4.1	5.40	6.38	3.59
k_z	17.5	16.84	18.07	16.13
k_v	25.8	27.64	30.83	29.31

[a] Isothermal values; isothermal-adiabatic correction is negligible.

bilities (Table V) within appropriately calculated tolerances.

Agreement with Kor's nominal value for c_{13} is not expected for it is extremely sensitive to the velocities. Kor calculates c_{13} from particular ELR velocities without first adjusting them to be compatible with the others. Consequently, our value for c_{13} is to be preferred.

c_{13}'s extreme sensitivity can be appreciated from the following formula:

$$c_{13}=\frac{\rho^2(v_{12a}{}^4+v_{14a}{}^4)-\rho^2(v_{9a}{}^4+v_{11a}{}^4)}{2c_{14}}-(c_{11}+2c_{44}),$$

where the symbols have their previously defined meanings. In principle, this expression can be used to calculate c_{13} directly, the extraneous root introduced by the quadratic already having been eliminated. We emphasize that properly calculated velocities and constants must be inserted unless one is willing to accept an uncertainty of 100% or more, and note that the value of c_{13} is, as it should be, independent of the convention used to determine the sign of c_{14} as the signs of the velocity function in the numerator and c_{14} change together. With this formula, it is necessary neither to employ the sign considerations outlined by Mayer and Parker[15] nor the conceivably less-discriminating strain-energy stability criteria.[16] An analogous expression for c_{13} in hexagonal systems, where c_{14} is identically zero, is not possible.

C. Elastic-Wave Refraction

In our attempt to understand v_{11}'s incompatibility for antimony, the 45° and 135° data were further analyzed in terms of the theory of plane elastic waves in aelotropic media.[17] Particle displacement and energy-flux directions, and the pure-mode direction in the Y-Z mirror plane, are calculated for both antimony and bismuth and compared with each other, and with the propagation and transducer-polarization directions. An outline of the calculation and the energy-flux expressions obtained are given in the Appendix; the results of this calculation, summarized in Fig. 2, are next discussed.

Our analysis shows that the unit displacement eigenvectors associated with the v_9 and v_{11} modes, A^9 and A^{11}, deviate by $-4°$ for antimony and $-5.2°$ for bismuth from the transducer polarization directions used to excite these modes. This small value is favorable for exciting the v_{11} mode in antimony, giving rise to the three well-defined pulses displayed by the oscilloscope. This same display obtains with either the 3-mm-diameter or the $\frac{1}{2}$-in.-square transducers. The corresponding deviations for A^{12} and A^{14} are $+14.6°$ for antimony and $+12.4°$ for bismuth. These deviations are not of a nature which would explain our egregious v_{11}, nor do the pure shear-mode directions in the Y-Z plane which are 117° for antimony and 107° for bismuth. However, the deviation of the energy flux, or ray velocity, from the normal is about 45°. For our dimensions, energy is deflected from a side before reaching the opposite reflecting face. Upon deflection the energy is refracted into spurious modes, giving rise to the pulses displayed. No pulse was found that corresponds with v_{11} calculated. This is due to the fact that in relation to the large intrinsic attenuation of antimony not enough energy flows along the wave-normal direction to reach the opposite face and to be echoed back to the transducer for detection.

We note that the smaller the flux deviation angle, the more numerous and better defined are the echoes, and that spurious pulses exist for almost every mode. Conical refraction effects along the triad axis, predicted by Waterman,[17] verified by Papadakis on rock salt and calcite,[18] and noticed by ELR in bismuth, did not interfere with obtaining decipherable echo patterns. For antimony the conical semi-angle in 28°40′; for bismuth, 32°30′.

Refraction effects were observed for either the 3-mm-diam or $\frac{1}{2}$-in-square transducers as sender-receiver. Many of the displays obtained with the larger one contained more spurious pulses than most displays obtained with the smaller one, depending apparently upon the propagation direction and the mode.

It is not possible for us to comment on the effects of the large deviation angles in bismuth since we do not have precise information on ELR's specimen geometry. We can only remark that the combined effects of specimen size, refraction, and attenuation are not as severe as they are in antimony. All of ELR's velocities are compatible and Eckstein[19] reports that his antimony echo displays are not as clean as they are for bismuth.

D. General Comments

Our experiment and analysis are based on plane elastic waves in extended media, and our specimens are

[15] W. G. Mayer and P. M. Parker, Acta Cryst. **14**, 725 (1961).
[16] G. A. Alers and J. R. Neighbors, J. Appl. Phys. **28**, 1514 (1957); L. J. Teutonico, *ibid.* **32**, 119 (1961).
[17] M. J. P. Musgrave, Proc. Roy. Soc. (London) **A226**, 339 (1954); P. C. Waterman, Phys. Rev. **113**, 1240 (1959); P. E. Borgnis, *ibid.* **98**, 1000 (1955); A. E. H. Love, *A Treatise on the Mathematical Theory of Elasticity* (Dover Publications, Inc., New York, 1944).
[18] E. Papadakis, J. Appl. Phys. **34**, 2168 (1963).
[19] Y. Eckstein (private communication).

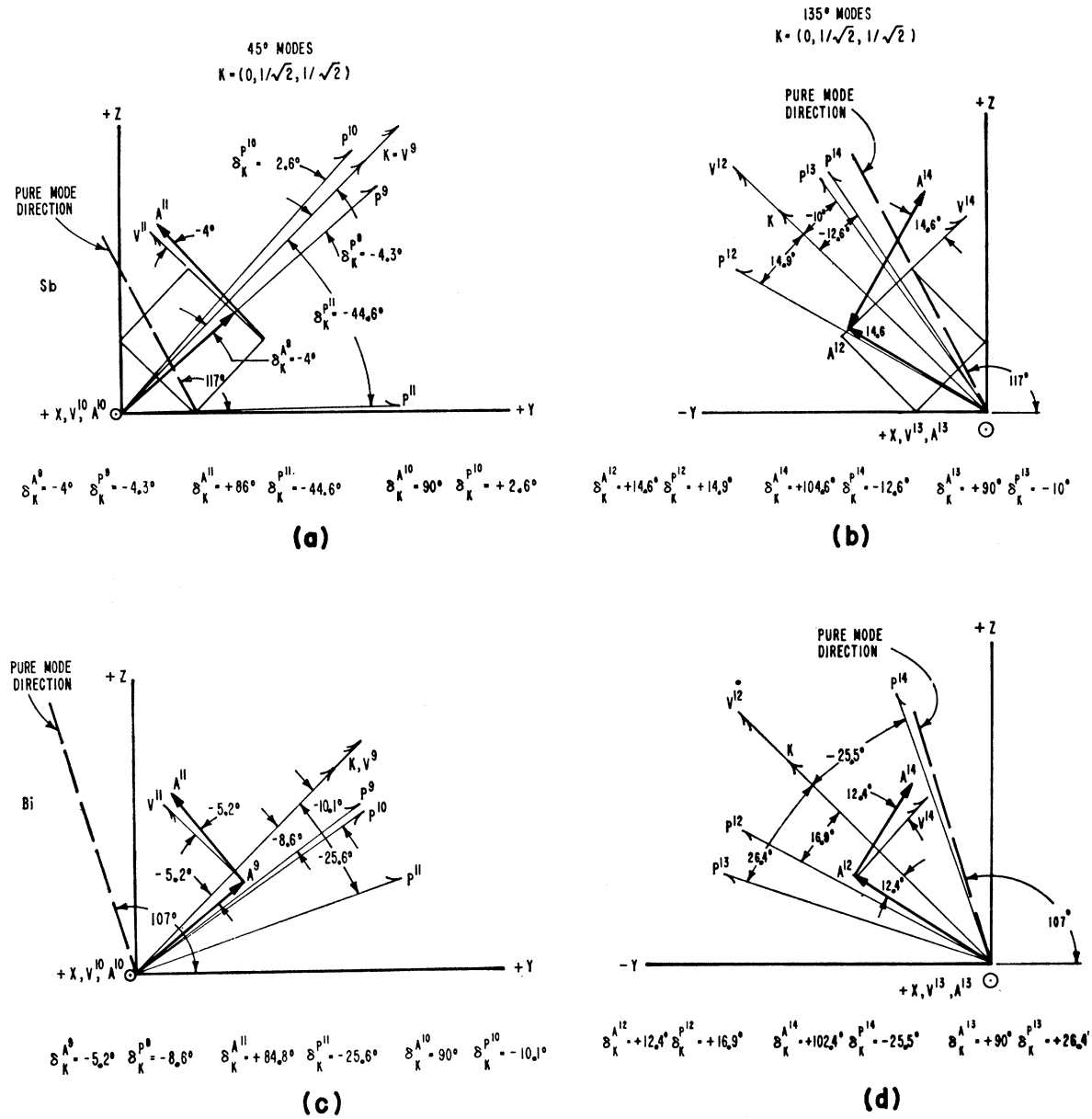

FIG. 2. Energy density flow, displacement, propagation and pure-mode directions in Y-Z mirror plane. $\delta_K{}^s$ is the angle between the vectors K and s where s is any of the vectors A^σ and P^σ. The signs for $\delta_K{}^s$ indicate placement at opposite sides of K with $+\delta$ counterclockwise. Parts (a) and (b) are for antimony, (c) and (d) for bismuth; (a) and (c) are for the 45° modes, and (b) and (d) for the 135° modes.

of finite dimensions. For isotropic circular bars the dilatational and distortional wave phase velocities have been shown by Pochhammer[20,21] to depend on the ratio of the cross section radius to wavelength a/λ and upon two functions of the Lamé stiffness constants. Chree[22] extended Pochhammer's results to noncircular, normal cross-sectioned cylinders and to nonisotropic media. In the absence of an exact treatment giving the longitudinal and two transverse phase velocities in anisotropic cubes it is reasonable to assume that the size of the correction for each phase velocity would be different. If these corrections are large in relation to the experimental errors, fitting the plane-wave formalism of redundancy eight to the 14 corrected velocities is not assured. That we are able to do so, however, suggests that the corrections are not significant. Our large minimum value of about 25 for k/λ, where k is the radius

[20] A. E. H. Love, *A Treatise on the Mathematical Theory of Elasticity* (Dover Publications, Inc., New York, 1944), p. 287.
[21] H. Kolsky, *Stress Waves in Solids* (Dover Publications, Inc., New York, 1963), p. 54.
[22] A. E. H. Love, *A Treatise on the Mathematical Theory of Elasticity* (Dover Publications, Inc., New York, 1944), p. 290.

of gyration of our noncircular section, suggests that these corrections would also be negligible for data with much narrower tolerances than we are able to specify. Our data cannot directly support this conclusion for it is possible that our large tolerances result in part from these effects.

Within the context of the above considerations, we believe our experiment to be a reasonable compromise as regards both the use of the plane elastic wave formalism in extended media for our finite sized specimens, and the use of predominantly energy-refracting modes in determining the elastic constants. Judging from the topological fitting procedure presented, we estimate that the values given are accurate to within about 5%.

APPENDIX I

In this section, we outline the general procedure used to calculate the energy flow components and present the expressions obtained for the 45° $(l,m,n::0,1/\sqrt{2},1/\sqrt{2})$ and 135° $(l,m,n::0,-1/\sqrt{2},1/\sqrt{2})$ propagation directions.

The ith Cartesian component of energy flow, P_i, is given by Love[19] as the negative of the scalar product of the component of the stress tensor on the surface normal to the ith direction, $\mathbf{T}_i$, with the particle displacement velocity $\dot{\mathbf{u}}$:

$$P_i=-\mathbf{T}_i\cdot\dot{\mathbf{u}}. \tag{A1}$$

The displacement

$$\mathbf{u}=p\mathbf{A}\exp(j(\omega t-\mathbf{K}\cdot\mathbf{r})) \tag{A2}$$

has components u_i where i runs from 1 to 3 corresponding to the x, y, z or x_1, x_2, x_3 directions. $\mathbf{A}$, $\mathbf{K}$, and $\mathbf{r}$ are in this order the particle displacement eigenvector of unit magnitude, the wave propagation vector, and the field point vector, and have components A_i, K_i, x_i. p is the scalar amplitude of the displacement; $\mathbf{T}_i$ has components X_{ij}, $j=1,2,3$. These are related in the usual way to the strains e_{rs} through the stiffness constants by

$$X_{ij}=c_{ijrs}(1+\delta_{rs})e_{rs}/2 \tag{A3}$$

summed for $r,s=1,2,3$; δ_{rs} is the Kronecker delta. In terms of the displacements,

$$e_{rs}=\left(\frac{\partial u_r}{\partial x_s}+\frac{\partial u_s}{\partial x_r}\right)\Big/(1+\delta_{rs}). \tag{A4}$$

For a particular mode g, the components of displacement, written as

$$u_i{}^g=p^gA_i{}^g\exp[j(\omega t-\mathbf{K}^g\cdot\mathbf{r})], \tag{A5}$$

are substituted into (A1) and (A4), and the result of substituting (A4) into (A3) in turn put into (A1). We finally obtain

$$P_i{}^g=\frac{-(p^g\omega)^2}{2v_g}c_{ijrs}A_j{}^gA_r{}^gl_s{}^g, \tag{A6}$$

where $l_s{}^g$, the cosine of the angle between $\mathbf{K}^g$ and the s coordinate axis, is l, m, or n for the gth mode, as $s=1$, 2, or 3. This expression is valid for crystals of any symmetry. It differs from Waterman's[18] Eq. (5.1) in that it is written directly in terms of the stiffness constants. (The four-index notation is reduced to the two-index notation in the usual way: $ij\rightarrow a$, $rs\rightarrow b$; $11\rightarrow 1$, $22\rightarrow 2$, $33\rightarrow 3$, $23=32\rightarrow 4$, $13=31\rightarrow 5$, $12=21\rightarrow 6$.)

Our results for $\mathbf{K}$ with direction cosines $(0,m,n)$ are the following: For $g=10$, $A^{10}=(1,0,0)$ for antimony and bismuth and

$$P_1{}^{10}=0, \tag{A7}$$

$$P_2{}^{10}=\frac{-(p^{10}\omega)^2}{2v_{10}}(mc_{66}+nc_{14}), \tag{A8}$$

$$P_3{}^{10}=\frac{-(p^{10}\omega)^2}{2v_{10}}(mc_{14}+nc_{44}). \tag{A9}$$

For $g=9$ and 11, we have $\mathbf{A}^9=(0,\ 0.7513,\ 0.6599)$, $A^{11}=(0,\ -0.6599,\ 0.7513)$ for antimony and $(0,\ 0.7696,\ 0.6385)$ and $(0,\ -0.6358,\ 0.7696)$ for bismuth; $m=n=1/\sqrt{2}$.

$$P_1{}^g=0, \tag{A10}$$

$$P_2{}^g=\frac{-(p^g\omega)^2}{2v_g}([mc_{11}-nc_{14}]A_2{}^gA_2{}^g+[-m2c_{14}+n\{c_{44}+c_{13}\}]A_2{}^gA_3{}^g+mc_{44}A_3{}^gA_3{}^g), \tag{A11}$$

$$P_3{}^g=\frac{-(p^g\omega)^2}{2v_g}([-mc_{14}+nc_{44}]A_2{}^gA_2{}^g+m[c_{44}+c_{13}]A_2{}^gA_3{}^g+nc_{33}A_3{}^gA_3{}^g). \tag{A12}$$

The appropriate $P_i{}^g$ for propagation in the $(0,\ -1/\sqrt{2},\ 1/\sqrt{2})$ direction follow from (A7)–(A12) by replacing $\pm m$ with $\mp m$, and the g indices 9, 10, 11 with 12, 13, and 14, respectively. The unit eigenvectors are $\mathbf{A}^{13}=(1,0,0)$, $\mathbf{A}^{12}=(0,\ -0.8625,\ 0.5060)$, $\mathbf{A}^{14}=(0,\ 0.5060,\ 0.8625)$ for antimony and $(1,0,0)$, $(0,\ -0.8421,\ 0.5393)$, $(0,\ 0.5393,\ 0.8421)$ for bismuth.

In the cases discussed, $P_1\equiv 0$, a result to be expected when the excitation does not disturb the mirror symmetry of the medium. The energy-flux deviation angle from the Z or X_3 axis, α, is $\tan^{-1}P_2/P_3$.

ACKNOWLEDGMENTS

The authors gratefully credit the following individuals for the contributions described: Dr. Joseph Trivissonno, John Carroll University, for initially setting up the experimental equipment and advising us on techniques during the early phase of its use; Dr. Allan J. Strauss, Lincoln Laboratory, MIT, for arranging for spark cutting, and Harry H. Ehlers, who did the cutting; Donald W. Eckart, USAEL, for assistance in checking specimen orientations and angles between cleavage

planes; Dr. Yakov Eckstein, Argonne National Laboratory, for general discussions, correspondence, and specific advice to make certain that the senses of the axes we used are the same as his; Arthur Ballato, USAEL, for general discussions; and Dr. D. I. Bolef, Washington University, and Dr. H. B. Huntington, Rensselaer Polytechnic Institute, for general comments.

We also owe thanks to Dr. L. J. Teutonico, Republic Aviation Corporation, and Dr. P. C. Waterman, AVCO Research Laboratory, for discussions on pure-mode and energy-flux directions in trigonal crystals; and Dr. Rudolf Bechmann and Dr. Erich Hafner, USAEL, for a critical review of the final manuscript, for stimulating and encouraging discussions on elastic-wave propagation.

Support of USAEL'S Institute for Exploratory Research and Solid State and Frequency Control Division, in the persons of Dr. H. H. Kedesdy, I. N. Greenberg, and F. A. Brand is indicated.

PHYSICAL REVIEW VOLUME 138, NUMBER 3A 3 MAY 1965

Critical Properties of the Heisenberg Ferromagnet with Higher Neighbor Interactions ($S=\frac{1}{2}$)

N. W. DALTON
Wheatstone Physics Laboratory, King's College, London, England

AND

D. W. WOOD
Department of Mathematics, University of Nottingham, Nottingham, England

(Received 21 September 1964; revised manuscript received 28 December 1964)

The method of exact power-series expansions has been extended to include both nearest-neighbor and next-nearest-neighbor interactions in the Heisenberg model. The series expansions for the susceptibility in zero magnetic field and the free energy in zero magnetic field have been derived to the fifth power in reciprocal temperature for the simple cubic, body-centered cubic, and face-centered cubic lattices. For the special case when all interactions are equal (equivalent-neighbor model), an additional term has been obtained in these expansions. For purposes of discussing the susceptibility and magnetic specific heat, the series expansions have been derived for lattices in which third-neighbor interactions are included, but only for the equivalent-neighbor model. Estimates of critical points are given, and the Padé-approximant method is used to study the dependence of the critical properties (temperature, energy, and entropy) on the relative strength of the first- and second-neighbor interactions. It is found that the variation in the critical point is well represented by

$$T_c(\alpha)=T_c(0)[1+m_1\alpha],$$

where $\alpha=J_2/J_1$ and lies in the range $0\leqslant\alpha\leqslant 1$, and $T_c(0)$ is the critical temperature of the nearest-neighbor model. The values of m_1 are 0.76, 0.99, and 2.74 for the fcc, bcc, and sc lattices respectively. Both the second-neighbor model and the equivalent-neighbor model are used to investigate the behavior of χ_0 for values of T near T_c. It is found that all the coefficients in the magnetic-specific-heat series expansion are positive for the equivalent-neighbor model, and that for lattices with large coordination numbers, reliable estimates of the critical point may be obtained using this function.

I. INTRODUCTION

MUCH previous work has been done on the critical behavior of the Heisenberg model of a ferromagnet when it is assumed that exchange interactions $(-2J\mathbf{S}_i\cdot\mathbf{S}_j)$ exist only between nearest-neighbor spins on the lattice. The most powerful theoretical approach towards obtaining estimates of critical constants is that introduced by Kramers and Opechowski.[1] In this method exact series expansions in ascending powers of reciprocal temperature are derived for the partition function and related thermodynamic functions for various lattice structures. In recent years much work has been done in extending the series expansions for the zero field susceptibility χ_0 and magnetic specific heat C_v to a high degree of approximation.[2] For the case where the spin variable S may take an arbitrary value the most extensive calculations have been performed by Rushbrooke and Wood.[3] These authors obtained the first six coefficients in the susceptibility series, and the first five coefficients in the magnetic specific-heat series. Recently a more powerful method of deriving these coefficients has been developed by

[1] H. A. Kramers, Commun. Kamerlingh Onnes Lab. Leiden, Suppl. No. 83. W. Opechowski, Physica 4, 181 (1937); 6, 1112 (1939).

[2] V. Zehler, Z. Naturforsch. **A5**, 344 (1950). H. A. Brown and J. M. Luttinger, Phys. Rev. **100**, 685 (1955). M. F. Sykes, thesis, Oxford, 1956 (unpublished). C. Domb and M. F. Sykes, Proc. Phys. Soc. (London) **B69**, 486 (1956).

[3] G. S. Rushbrooke and P. J. Wood, Proc. Phys. Soc. (London) **A68**, 1161 (1955); Mol. Phys. **1**, 257 (1958).